MICROWAVE OPERATION OF InGaAs/InAlAs CHARGE INJECTION TRANSISTORS

P. M. Mensz,§ H. Schumacher,† P. A. Garbinski, A. Y. Cho, D. L. Sivco, and S. Luryi

AT&T Bell Laboratories, Murray Hill, NJ 07974, USA
† Bell Communications Research, Red Bank, NJ 07701

ABSTRACT

Charge injection transistors, implemented in an InGaAs/InAlAs/InGaAs heterostructure lattice-matched to InP, were characterized on-wafer at room temperature in a frequency range 0.5 – 25.5 GHz. The differential current gain (h_{21}) and the maximum available power gain (MAG) were calculated from the measured scattering S-parameters and plotted against frequency for a number of DC biasing conditions. The high-frequency rolloff was slower than 20 dB/decade for both h_{21} and the MAG. Extrapolating the experimental gain data at 20 dB/decade, we concluded that the unity current gain is above 40 GHz. The MAG $\gg 1$ was measured up to 25 GHz and its extrapolated cut-off frequency is higher than 35 GHz.

INTRODUCTION

The charge-injection transistor (CHINT) is a three-terminal heterostructure device [1], [2] based on the real-space transfer (RST) of hot electrons between two conducting layers. One of these layers ("emitter") has source and drain contacts and plays the role of a hot-electron cathode. The other layer ("collector") is separated by a potential barrier. When the emitter electrons are heated by the source-drain field most of them do not reach the drain but are injected over the barrier into the collector layer; a strong negative differential resistance (NDR) develops in the drain circuit. A number of functional elements have been contemplated [3], based on the unique characteristics of three-terminal RST devices. The efficient control of hot-electron injection (the CHINT action) allows the implementation of novel circuit elements. In particular, we have demonstrated a device structure that performs such logic operations as *NOR* and *AND* with a controlled switching between these functions [4].

High-frequency characterization has been reported for CHINT devices implemented in GaAs/AlGaAs heterostructures [5] and, recently, for a novel three-terminal RST device in a strained-layer InGaAs/AlGaAs/GaAs heterostructure [6]. The InGaAs/InAlAs system lattice-matched to InP, despite its obvious advantages for RST transistors, had been off-limits for a long time because of the difficulties in implementing non-shorting ohmic contacts. Recently, these problems have been overcome with the help of non-alloyed epitaxial contacts [7]. The improved RST transistors [8] showed an outstanding DC performance at room temperature: the transconductance of controlled charge injection exceeding 23 Siemens per mm of emitter width and the NDR peak-to-valley ratio approaching 10^4.

The present work reports our microwave characterization of InGaAs/InAlAs/InGaAs CHINT devices up to a frequency $f = 25.5$ GHz. In this experiment we used devices identical with the ones reported in ref. [8], where details of the device structure and fabrication procedure can be found. The data presented throughout this work originate from the same device.

STATIC CHARACTERISTICS

The basic device structure is sketched in the inset to Fig. 1. The active area of the device represents a strip of the emitter layer 9.5 μm long and 50 μm wide. The channel is defined by a 0.8 μm long trench etched into the n^+ cap layer between the source and drain.

Figure 1 displays the drain (I_D) and the collector (I_C) characteristics as a function of the heating voltage V_D at a constant collector bias $V_C = 4.0$ V. This measurement was obtained prior to the microwave testing using a semiconductor parameter analyzer HP4145B and on-wafer testing by low-inductance "Cascade Microtech" probes and a Model 42 probe station. The low-inductance probes substantially reduce the circuit oscillations at

§ Current address: Philips Laboratories, Briarcliff Manor, NY
† Current address: University of Ulm, D-7900 Ulm, Germany

CH2865-4/90/0000-0323 $1.00 © 1990 IEEE

low frequency caused by the NDR in the drain circuit. The device shows a strong negative differential conductance with the peak-to-valley ratio exceeding 30, and a high CHINT transconductance (defined by $g_m \equiv \partial I_C/\partial V_D$ at constant V_C) that reaches 2.3 Siemens/mm at $V_D = 1.24$ V.

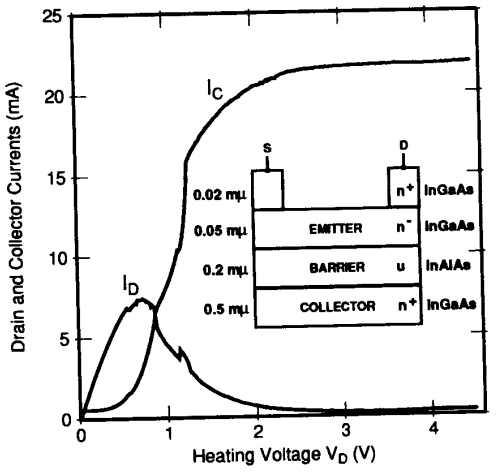

Figure 1: Basic *I-V* characteristics of the device used for microwave characterization. The device structure is schematically shown in the inset.

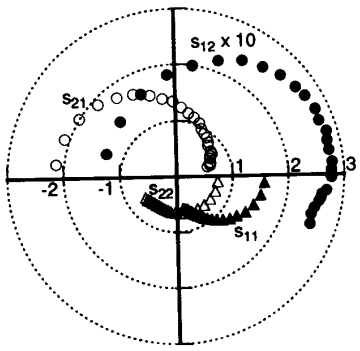

Figure 2: Measured scattering parameters at $V_C = 4.0$ V and $V_D = 0.8$ V. The S-matrix data are plotted on the complex plane in the frequency range from 0.5 to 25.5 GHz.

MICROWAVE RESULTS

We characterized the high-frequency operation of CHINT devices using a HP8510B network analyzer. The HP4145 parameter analyzer suplied the DC bias to the device through a broad-band bias tee. The device was operated in the common-source configuration, with the input signal applied to the drain and the output signal taken from the collector. The setup was calibrated using an impedance-standard substrate.

Figure 2 displays the S-parameter data on a complex plane. These data were obtained at $V_C = 4.0$ V and $V_D = 0.8$ V, which corresponds to a region immediately following the onset of NDR in the drain characteristic (Fig. 1). Compared to bipolar or field-effect transistors, the S-parameters of CHINT show several unusual features. In particular, $\arg(S_{12}) \rightarrow \pi$ in the DC limit, which suggests the existence of a positive feedback. Also, the magnitude of the input reflection coefficient $|S_{11}|$ can be larger than unity due to the NDR in the input circuit. On the other hand, the behavior of S_{21} and S_{22} shows no apparent anomalies.

From the scattering parameters, we calculated the small-signal current gain, h_{21}, and the maximum available gain (MAG). The frequency dependences of the small-signal gain parameters are shown in Fig. 3 for a number of bias conditions. In the range of frequencies where Rollet's factor K is less than unity, the maximum stable gain (MSG) was calculated instead of MAG. At these frequencies, the device is potentially unstable. Since in the range where MAG exists ($K > 1$) it equals $\text{MSG} \times [K - (K^2 - 1)^{1/2}]$, the composite MSG/MAG curves exhibit a kink near $K = 1$. For some bias conditions, e.g., for $V_D = 1.10$ V and $V_C = 4.5$ V, the device is potentially unstable up to the highest measured frequencies and the corresponding curve (labeled d_2 in Fig. 3b) has no kink.

In general, the high-frequency rolloff of the gain parameters in our device has a slope smaller than 20 dB/decade. The variations in the slope of the rolloff with the bias conditions are weaker for MSG and MAG than for h_{21}. Extrapolating at 20 dB/decade (as shown in Fig. 3a by a dashed line), we find that the highest unity-current-gain frequency is slighty above 40 GHz. The maximum oscillation frequency, f_{MAX}, is difficult to obtain for bias points where MAG does not exist within the measurement range, i.e. if $K < 1$ for $f \leq 25.5$ GHz. As can be seen from Fig. 3b at $V_D = 1.10$ V and $V_C = 4.5$ V, the device still oscillates ($K = 0.68$) at $f = 25$ GHz. Extrapolating from the frequency

dependence of the K-factor, we find that K approaches unity at $f \approx 35$ GHz, which gives a conservative estimate for the f_{MAX} in our device.

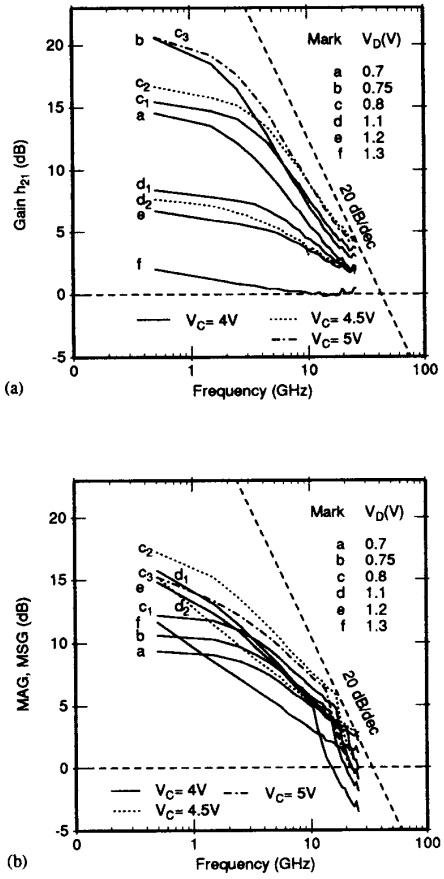

Figure 3: Small-signal gain parameters calculated from the measured S-parameters at different DC bias conditions.
(*a*) Frequency dependence of the current gain h_{21};
(*b*) Frequency dependence of the power gain parameters (MSG or MAG). The MSG is plotted in the frequency range where $K < 1$ and the MAG is not defined. When $K \geq 1$, the displayed data represent the MAG.

Figure 4 shows the dependence of the small-signal gain parameters on the DC bias conditions. The plotted data correspond to the low-frequency limit (0.5 GHz) and illustrate an interesting point peculiar to CHINT. Because of the vanishing differential input conductance at the onset of the NDR, the magnitude of the gain exhibits a pronounced peak in this region. If we were to plot the data including the phase factor, the variation of gain would be of a "dispersive" shape.

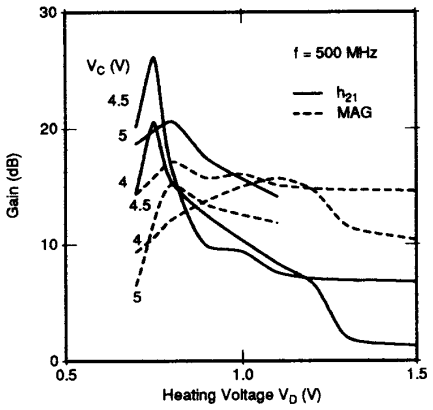

Figure 4: Dependence of the small-signal gain parameters on DC bias conditions.

CONCLUSION

The charge injection transistor is attractive for high speed electronics since its ultimate performance is believed to be limited only by the time of flight of hot electrons across the barrier layer (another delay associated with the time required to establish an electron temperature in the emitter channel is expected to be shorter than 1 picosecond) [3,9]. For our present device with a 2 000 Å thick barrier the transit time can be estimated to be between 2 and 3 ps. This would mean an f_T between 50 and 80 GHz. Inasmuch as the bandwidth of our devices is below this fundamental limitation, it is likely that the RC delay associated with the parasitic drain-to-collector capacitance is still responsible for limiting the device speed, just as it was the case for devices used in earlier microwave studies [5].

One obvious direction for improvement is to minimize the drain area. However, since the transit time decreases while the *RC* delay increases with diminishing barrier thickness, the drain-to-collector capacitance will always remain a factor to be concerned about. An interesting alternative approach was recently reported by Hueschen et al. [6]. These authors studied an RST transistor, very similar in concept to CHINT, but with an inverted structure in which the collector is the top layer. This allowes to reduce the drain-collector capacitance, which has probably contributed to the higher current-gain cutoff frequency (f_T = 60 GHz) found in ref. [6]. On the other hand, the unity-gain frequency for the MAG was somewhat lower (18 GHz). These results are promising and a comparison of the two approaches would be very interesting; we are unable to pursue such an analysis at this time because Hueschen et al. [6] have not reported the DC characteristics of their device.

ACKNOWLEDGEMENTS

We are grateful to M. Fang and A. Kastalsky for discussions and helpful advice.

REFERENCES

1. A. Kastalsky and S. Luryi, "Novel Real-Space Hot-Electron Transfer Devices", *IEEE Electron Device Lett.* **EDL-4**, 334 (1983).
2. S. Luryi, A. Kastalsky, A. C. Gossard, and R. H. Hendel, "Charge Injection Transistor Based on Real-Space Hot-Electron Transfer", *IEEE Trans. Electron Devices* **ED-31**, 832 (1984).
3. S. Luryi and A. Kastalsky, "Hot electron injection devices", *Superlattices and Microstructures* **1**, 389 (1985).
4. S. Luryi, P. M. Mensz, M. R. Pinto, P. A. Garbinski, A. Y. Cho, D. L. Sivco, "Charge Injection Logic", *Appl. Phys. Lett.* **57**, October 22 (1990). This letter contains references to the recent literature on RST transistors.
5. A. Kastalsky, J. H. Abeles, R. Bhat, W. K. Chan, and M. Koza, "High-Frequency Amplification and Generation in Charge Injection Devices", *Appl. Phys. Lett.* **48**, 71 (1986).
6. M. R. Hueschen, N. Moll, and A. Fischer-Colbrie, "Improved Microwave Performance in Transistors Based on Real-Space Electron Transfer", *Appl. Phys. Lett.* **57**, 386 (1990).
7. P. M. Mensz, S. Luryi, A. Y. Cho, D. L. Sivco, and F. Ren, "Real Space Transfer in Three-Terminal InGaAs/InAlAs Heterostructure Devices", *Appl. Phys. Lett.* **56**, 2563 (1990).
8. P. M. Mensz, P. A. Garbinski, A. Y. Cho, D. L. Sivco, and S. Luryi, "High Transconductance and Large Peak-To-Valley Ratio of Negative Differential Conductance in Three-Terminal InGaAs/InAlAs Real-Space Transfer Devices", *Appl. Phys. Lett.* (1990).
9. I. C. Kizillyalli and K. Hess, "Physics of Real-Space Transfer Transistors", *J. Appl. Phys.* **65**, 2005 (1989).